gel thus formed is reactive toward $Ba(OH)_2$ under ambient conditions and results in formation of an amorphous $BaTiO_3$-like structure. (c) $Ba(OH)_2$ is unreactive toward anatase until 450 °C, when it forms Ba_2TiO_4 and finally $BaTiO_3$ between 700 and 900 °C. (d) The complex formed by reaction of $Ba(OH)_2$ and TiO_2 gel evolves to Ba_2TiO_4, $BaTiO_3$, and a mixture of $BaTiO_3$ and $BaTi_2O_5$ upon heating the 2:1, 1:1, and 1:2 Ba/Ti ratio materials.

Second-Order Nonlinear Optical Properties of N-(4-Nitrophenyl)-(s)-prolinol-Doped Sol–Gel-Processed Materials

Yue Zhang and Paras N. Prasad*

Photonics Research Laboratory, Department of Chemistry, State University of New York at Buffalo, Buffalo, New York 14214

Ryszard Burzynski

Laser Photonics Technology, Inc., Baird Research Park, 1576 Sweet Home Road, Amherst, New York 14228

The sol–gel-processing technique has been used to prepare a new material for nonlinear optics. The second-order nonlinear optically active molecule N-(4-nitrophenyl)-(s)-prolinol has been doped to an inorganic oxide matrix in relatively high concentration. Electric field poling was successfully employed to introduce noncentrosymmetry required for second-order nonlinearity. Studies using in situ poling allowed the formulation of conditions under which stable poled orientation was achieved. Second harmonic generation and electrooptic modulation studies have been conducted on this material.

Introduction

The application of nonlinear optical processes to photonics has drawn great interest to the search for new nonlinear optical (NLO) materials.[1-3] These applications require high optical quality materials with low dielectric constant, high optical damage threshold, and high and stable optical nonlinearities. Organics are promising nonlinear optical materials because their molecular structure can be tailored to achieve large optical nonlinearity. They also offer advantages over inorganic materials in material processing and fabrication in the form of thin films, optical fibers, and optical wave guides, etc.

For applications involving second-order nonlinear optical processes, a stringent symmetry requirement is imposed upon the materials, i.e., the active molecular units must be arranged in a noncentrosymmetric fashion to show nonzero second-order nonlinear coefficients. Single crystals with proper symmetry, grown from both inorganic and organic materials, have been shown to perform effectively in second-order nonlinear optical processes. For organic polymers and polymeric materials fabricated in the form of thin films, the noncentrosymmetry is achieved by electric field poling.[4] In this process, a strong electric field is applied across the material to orient the molecules, with nonzero dipole moments, in the direction of the electric field. Conventionally, nonlinear optically active groups are either attached to polymer backbones or simply doped into polymers.[4,5] In both cases, the fast relaxation of the nonlinear optical units back to random orientation prevents these materials from practical applications. Pure polymers doped with nonlinear optically active molecules often do not form good-quality films. Different methods have been proposed to improve the optical quality of these materials and to achieve stable second-order nonlinear

optical coefficients. For example, Ye et al. showed that hydrogen bonding can lead to a considerable increase in stability by establishing a weak cross-linked network.[6] Robello et al.[7] and Eich et al.[8] showed that cross-links in multifunctional acrylic systems and diepoxide-diamine condensation reactions, respectively, can also lead to considerable increase in the stability of poled structures. A major concern using this approach is the loss of optical quality.

Sol–gel processing is a technique which enables the preparation of amorphous or crystalline inorganic oxides starting from solutions of suitable precursor compounds, usually alkoxides, through their reaction with water.[9] This technique offers many advantages for material processing,[10,11] among them the inorganic–organic composite

(1) Prasad, P. N.; Williams, D. J. *Introduction to Nonlinear Optical Effects in Molecules and Polymers*; John Wiley & Sons: New York, 1991.

(2) Chemla, D. S., Zyss, J., Eds. *Nonlinear Optical Properties of Organic Molecules and Crystals*; Academic Press: Orlando, FL, 1987.

(3) Williams, D. J., Ed. *Nonlinear Optical Properties of Organic and Polymeric Molecules*; ACS Symp. Ser. No. 233; American Chemical Society: Washington, DC, 1983.

(4) Singer, K. D.; Kuzyk, M. G.; Sohn, S. E. In *Nonlinear Optical and Electroactive Polymers*; Prasad, P. N., Ulrich, D. R., Eds.; Plenum Press: New York, 1988.

(5) Willand, C. S.; Feth, S. E.; Scozzafava, M.; Williams, D. J.; Green, G. D.; Weinschenk, J. I., III; Hall, H. I., Jr.; Mulvaney, J. E. In *Nonlinear Optical and Electroactive Polymers*; Prasad, P. N., Ulrich, D. R., Eds.; Plenum Press: New York, 1988.

(6) Ye, C.; Marks, T. J.; Yang, J.; Wong, G. K. *Macromolecules* **1987**, *20*, 2324.

(7) Robello, D. R.; Ulman, A.; Willand, C. S.; Williams, D. J. U.S. Patent 4796971, 1989.

(8) Eich, M.; Reck, B.; Toon, D. Y.; Wilson, C. G.; Bjorklund, G. C. *J. Appl. Phys.* **1989**, *66*, 3241.

(9) Klein, L. C., Ed. *Sol-gel Technology for Thin Films, Fibers, Preforms, Electronics and Specialty Shapes*; Noyes Publications: Park Ridge, New Jersey, 1988.

(10) Zhang, Y.; Prasad, P. N.; Burzynski, R. *Proceedings of the Conference on Ultrastructures*; Orlando, FL. 1991; John Wiley: New York, in press.

---

*Author for correspondence.

material preparation. Composite components of inorganic oxides and organics can be mixed in virtually any ratio necessary to obtain the desired properties. This makes the composites extremely versatile in their composition, processing, and optical and mechanical properties. The components are combined in a liquid phase, ensuring that the final products be homogeneous. Second-order nonlinear optically active organic molecules can be easily doped into the oxide matrix and electrically poled before the full densification of the glass. Heat treatment while the poling field is kept on may lock the molecules in a preferable direction and stable second-order nonlinearity can be achieved.

We report in this paper the preparation of a new second-order (NLO) material processed by the sol–gel technique. N-(4-Nitrophenyl)-(s)-prolinol (NPP), with a β value of 86.2×10^{-30} esu,[12] was doped to the inorganic oxides (SiO_2 and TiO_2) matrix in relatively high concentration (15 wt %). Electric field poling was employed to align the NPP molecules. In situ poling measurements enabled us to find the optimal conditions to achieve large and stable second-order nonlinearity without the loss of optical quality. Second-harmonic generation and electrooptic modulation experiments have been conducted on this material. High second-order susceptibility with long-term stability has been obtained.

Experiments and Results

Material Processing and Poling. Sol–gel matrix preparation essentially follows the recipe reported by Weisenbach et al.[13] and Roncone et al.[14] Prehydrolyzed tetraethoxysilane (TEOS) sol was mixed with the titania precursor (titanium butoxide) in a molar ratio of 1:1. Different solvents of good wetting properties and relatively low vapor pressure were used to achieve the best uniformity of the spin-coated films. The blend of alkoxides was left stirring to allow the titania precursor to hydrolyze. NPP solution was mixed with the alkoxides while stirring. Different amounts of NPP were incorporated in the sol–gel matrix, but detailed studies were conducted only on the samples containing the highest NPP concentration (15 wt %). The final solution was stirred for several hours to ensure a homogeneous mixing.

For corona poling second-harmonic generation (SHG), the sol–gel film was cast on a regular glass substrate prewetted by proper solvents (normally isopropyl alcohol). Corona poling[4] was performed by applying a high dc voltage of 5 kV to a tungsten wire (25 μm in diameter) located 8 mm above the grounded base electrode on which the NLO films were placed. For contact plate poling second-harmonic generation and electrooptic (EO) modulation, the film was spin-coated on the ITO coated glass substrate. Spin speed was controlled such that the film thickness was around 1 μm. The film thickness was confirmed by using a profilometer. A set of circular silver thin films (3 mm in diameter) was then vacuum deposited on the top of the sol–gel composite film. These silver films act as both electrodes and mirrors. Poling was done by applying a dc voltage of about 100 V to the silver electrodes
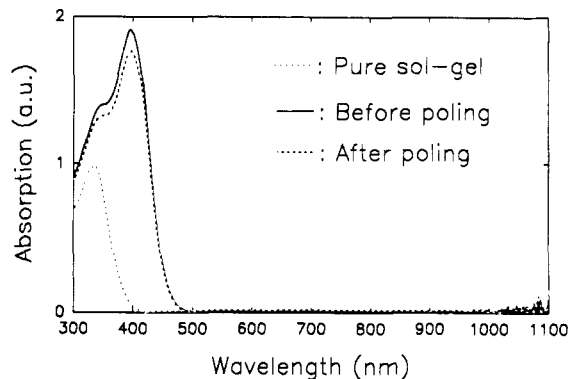
(11) Zhang, Y.; Cui, Y. P.; Wung, C. J.; Prasad, P. N.; Burzynski, R. *Proc. SPIE* **1991,** *1560,* 264.

(12) Zhang, Y.; Lee, K. S.; Ghosal, S.; Prasad, P. N., manuscript in preparation.

(13) Weisenbach, L.; Davis, T. L.; Zelinski, B. J. J.; Roncone, R. L.; Weller-Brophy, L. A. In *Better Ceramics Through Chemistry IV;* Zelinski, B. J. J., Brinker, C. J., Clark, D. E., Ulrich, D. R., Eds.; Materials Research Society: Pittsburgh, 1990; p 377.

(14) Roncone, R. L.; Weller-Brophy, L. A.; Weisenbach, L.; Zelinski, B. J. *J. Non-Cryst. Solids* **1991,** *128,* 111.
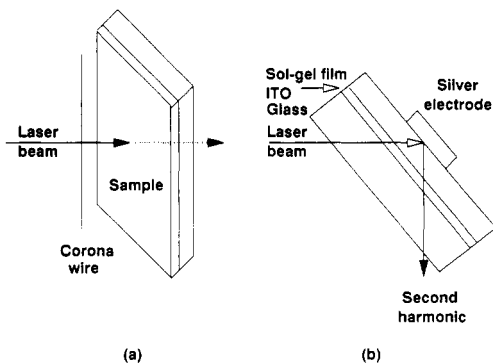

Figure 1. Absorption spectra of the sol–gel/NPP film before and after poling along with the absorption spectrum of the pure sol–gel film.

with the ITO conducting layer grounded.

Linear Optical Properties. The absorption spectra were recorded using a Shimadzu UV–vis spectrometer. The spectra of the sol–gel/NPP film before and after poling are presented in Figure 1. Also shown is the absorption spectrum of a pure sol–gel film. The films show no absorption at the fundamental (1.064 μm) or the harmonic (532 nm) wavelength. The refractive indexes of the film measured at 1.064 μm, 633 nm and 532 nm using the waveguide coupling technique are, respectively, 1.591, 1.605, and 1.620.

Poling Dynamics and Second-Harmonic Generation. The poled material possesses the ∞mm point group symmetry. This symmetry reduces the nonvanishing components of the macroscopic susceptibility to $\chi_{zzz}^{(2)}$ and $\chi_{zxx}^{(2)}$ which, to the first order of the poling electric field, are related to the microscopic hyperpolarizability, β, by

$$\chi_{zzz}^{(2)}(-2\omega;\omega,\omega) = fN\mu\beta E_{\mathrm{p}}/5kT \qquad (1)$$

$$\chi_{zzz}^{(2)} = 3\chi_{zxx}^{(2)} \qquad (2)$$

where $f = f^{2\omega}(f^{\omega})^2 f^0$ is the local field factor, μ is the molecular dipole moment, E_{p} is the poling electric field, and kT is the thermal energy.

The second-harmonic intensity generated from the poled film is given by

$$I_{2\omega} = \frac{512\pi^3}{A} t_\omega{}^4 T_{2\omega} d^2 t_0{}^2 p^2 I_\omega{}^2 \frac{1}{(n_{2\omega}{}^2 - n_\omega{}^2)^2} \sin^2 \Psi(\theta) \qquad (3)$$

where A is the area of the laser beam spot; d is the appropriate second harmonic coefficient in the contracted notation; t_ω, $T_{2\omega}$, and t_0 are transmission factors;[4] I_ω is the fundamental laser intensity; p is the angular factor which projects the nonlinear susceptibility tensor onto the coordinate frame defined by the propagating electric field, and n's are the refractive indexes at the appropriate frequencies. The angular dependence term, $\Psi(\theta)$, of the second harmonic intensity can be expressed as

$$\Psi(\theta) = (\pi L/2)(4/\lambda)(n_\omega \cos \theta_\omega - n_{2\omega} \cos \theta_{2\omega}) = \pi L/2l_c \qquad (4)$$

where $l_c = \lambda/4(n_\omega \cos \theta_\omega - n_{2\omega} \cos \theta_{2\omega})$ is the coherence length. At normal incidence, $l_c = \lambda/4(n_\omega - n_{2\omega})$.

One of the features of the sol–gel-processed materials doped with NLO molecules is that poling can be done even at room temperature before the glass matrix is fully densified. This process takes advantage of high mobility of the molecules in the pores of the composite sol–gel matrix. Subsequent heat treatment of the film causes the pores to shrink and thus locks the molecules in the poled orientation. In situ poling under various conditions has been

Nonlinear Optics of Sol-Gel Processed Materials

Chem. Mater., Vol. 4, No. 4, 1992 853

Figure 2. Experimental configurations for corona poling (a) and for contact plate poling (b) second harmonic generation.
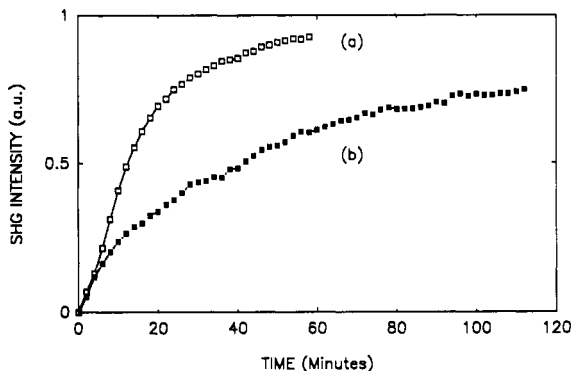

Figure 4. Dependence of the second harmonic intensity on the electric field, E_p. The square root of $I_{2\omega}$ is plotted against E_p.

Figure 3. Second-harmonic buildup in a sol–gel film doped with NPP: (a) corona poling at room temperature; (b) contact plate poling at room temperature.

Figure 5. Decay of the second harmonic intensity as the poling voltage is turned off: (a) poling voltage off immediately after the film was heated to 115 °C; (b) voltage off after 1 h heating at 115 °C and then cooled to 70 °C; (c) voltage off after 3 h of heating at 115 °C and then cooled to room temperature.

conducted by monitoring the second harmonic intensity while the poling voltage is applied and turned off. The experimental setup was similar to that described previously.[11] The second harmonic measurement was carried out with a Q-switched, mode-locked Nd:YAG laser operating at 500 Hz, with a pulse train consisting of 40 sub-pulses at 1.06 μm and with each pulse 135 ps wide. The second harmonic signal was detected by a Hamamatsu photomultiplier tube (PMT, Model 2014) and processed by an EG&G Boxcar averager. Both corona poling and contact plate poling were used and compared. In the first case, the corona poling setup was placed in the laser beam at 45° to film normal, and the transmitted second harmonic was detected (see Figure 2a). In the case of contact plate poling, the film, coated on the ITO layer and with silver electrodes on it, was placed in the laser beam in such a way that the reflected second harmonic signal could be monitored (see Figure 2b). In both cases, a p-polarized fundamental laser beam was used and the p component of the second harmonic signal was measured.

Figure 3 shows the SH signal buildup after the poling field is applied at room temperature, for both corona poling and contact plate poling. It clearly indicates that the molecules can be efficiently poled even at room temperature. As one can see, the reflection second-harmonic intensity rises much slower, when a dc poling voltage of 100 V is applied (Figure 3a), compared to the second harmonic intensity in the case of corona poling (Figure 3b). This implies that contact plate poling is not as efficient as corona poling and results in a smaller $\chi^{(2)}$ value. One sees from eq 1 that the second-order susceptibility is linearly proportional to the applied electric field. This is true only under week electric field and the equation must be modified in the case of a strong field. As a test, we monitored this dependence by poling the NLO material with different voltages and detecting the second harmonic intensity after
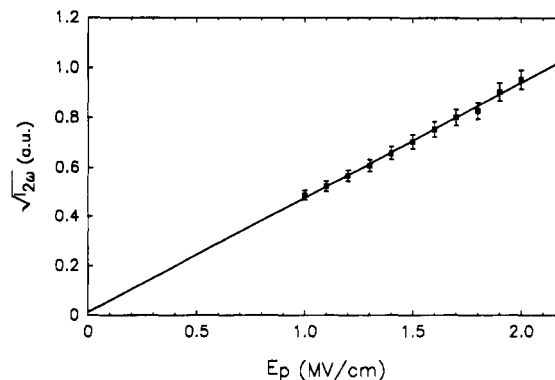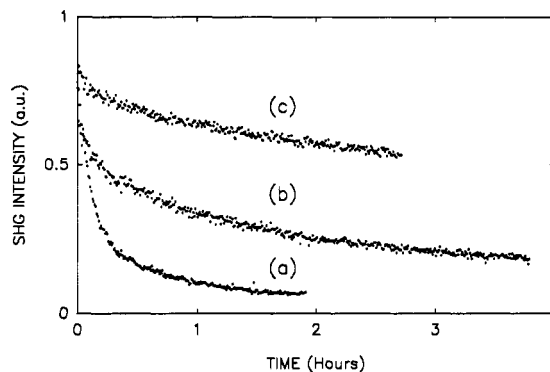
the poling field was removed. The maximum field applied was 2×10^6 V/cm; higher fields resulted in the dielectric breakdown of the film. A linear dependence of the measured $\chi^{(2)}$ value on the applied field was obtained, as shown in Figure 4, where the square root of the second-harmonic intensity, proportional to the second-order susceptibility, is plotted.

The influence of heat treatment of the sol–gel/NPP film on the stability of the second-order nonlinearity was also studied. Films made from the same material under same conditions were heated to different temperatures and for different periods of time. The decay of the SH signal after heating the film to 115 °C and cooling to different temperatures was monitored. Curve a in Figure 5 depicts the SH signal when the poling voltage was turned off immediately after the film was heated to 115 °C. The relatively fast decay of the SH intensity indicates that the NPP molecules still have freedom to relax back to a random orientation. Longer heat treatment apparently locks the molecules in the direction of the electric field and thus reduces the decay rate of the SH signal, as shown in Figure 5b,c.

After the optimum poling conditions were found, a new 1-μm-thick film was cast on the glass substrate and left at room temperature for several hours to allow the solvent to evaporate. It was then placed in the corona poling setup. A dc voltage of 5 kV was applied to the tungsten wire followed by heating the film to 115 °C at a rate of 20–40 °C/h and kept at this temperature for 5 h. After this step, the film was cooled to room temperature, and the dc voltage was turned off.

The second-order nonlinearity of the material was measured using the angular dependence method. The film, after poling, was placed on a rotational stage and was
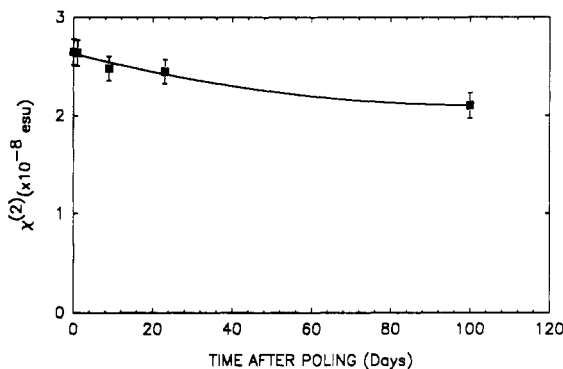
Figure 6. Long-term decay of the second-order susceptibility, $\chi^{(2)}(-2\omega;\omega,\omega)$, after poling.
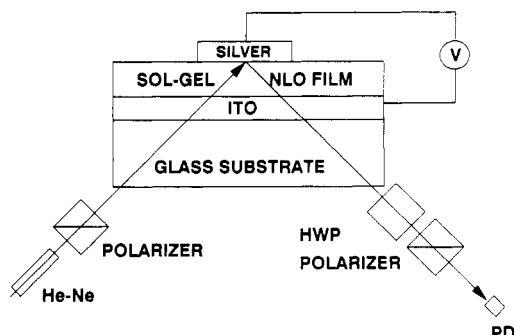

Figure 7. Experimental setup for the electrooptic modulation.

rotated around an axis perpendicular to the laser beam. The fundamental laser beam was p polarized, and only the p component of the SH signal was detected. The SH signal was recorded as a function of the rotation angle. Since the film thickness is much smaller than the coherence length of the material, only the envelope of the Maker fringes could be observed. This envelope was computer fitted to find the amplitude and the angle of maximum intensity. The second-order susceptibility $\chi^{(2)}$ was evaluated by comparing the maximum SH intensity to that obtained from an X-cut quartz crystal.[15] A $\chi^{(2)}$ value of 2.6×10^{-8} esu was obtained immediately after poling.

This procedure was repeated for a period of more than 3 months. The measured long-term decay of $\chi^{(2)}$ after poling is presented in Figure 6. After more than 3 months, the $\chi^{(2)}$ value dropped less than 20% of the original value.

Electrooptic Modulation. To perform the electrooptic modulation experiment, the sol–gel film was cast on the ITO coated glass substrates. A group of circular thin silver films was vacuum deposited onto the sol–gel film. Poling was done by applying a dc voltage of 100 V to the silver electrodes with the ITO layer grounded. The experimental setup is shown in Figure 7. A He–Ne laser beam polarized 45° with respect to the plane of incidence passes through the ITO layer, traverses the sol–gel film, and then is reflected by the silver electrode. The second polarizer analyzes the outgoing laser beam from the film. A quarter-wave plate was used to introduce a $\pi/2$ phase shift. A Kepco BOP-500M power supply provided the dc poling voltage as well as the modulating ac voltage by amplifying a small ac voltage from a wave signal generator. The modulated light signal was detected by a photodiode, amplified using a home-made preamplifier (500 amplification ratio), displayed and measured with the help of an oscilloscope.

When an alternating voltage is applied across the poled sol–gel/NPP film, the laser beam has its phase modulated

due to the material's birefringence induced by poling. Because the poled film possesses an ∞mm symmetry, the only nonzero components of the electrooptic coefficients are r_{31} and r_{33} with $r_{33} = 3r_{31}$ according to Kleinman's symmetry argument. These coefficients are determined by measuring the ratio, Γ_m, between the modulated light intensity (ac) to the unmodulated light intensity using the following equations:[16]

$$\Gamma_m = \frac{2\pi}{\lambda} h \Delta n_0 \frac{\sin^2 \theta}{\cos \theta} \tag{5}$$

$$\Delta n_0 = \frac{1}{2}(n_3{}^3 r_{33} - n_1{}^3 r_{31}) V/h \tag{6}$$

where h is the thickness of the film, Δn_0 is the birefringence one would measure if the light traversed the length of the film, λ is the laser wavelength, and θ is the angle of incidence. n_1 and n_3 are the refractive indexes along the directions perpendicular and parallel to the poling electric field, respectively, and r_{31} and r_{33} are the Pockels' coefficients corresponding to the off-diagonal and diagonal terms. Finally, these coefficients are related to the second-order susceptibility by

$$\chi_{zzz}^{(2)}(-\omega;\omega,0) = -n^4 r_{33}/8\pi \tag{7}$$

The electrooptic modulation experiment was performed on a 1-μm-thick poled sol–gel processed $SiO_2/TiO_2/NPP$ film at a frequency of 1.59 kHz. The ac modulating voltage used was 100 V peak to peak. The measured $\chi_{zzz}^{(2)}(-\omega;\omega,0)$ using a He–Ne laser operating at 632.8 nm was 5×10^{-9} esu.

Discussion and Conclusion

We have conducted in situ poling second harmonic generation measurements to find the optimum conditions for obtaining long-term stable second-order nonlinearity. Our results show that, for the sol–gel processed inorganic oxides:organic molecules composites, the NLO molecules can be reoriented easily at room temperature. The poling electric field should be applied before the heat treatment which causes the pores of the oxide matrix to shrink and, consequently, immobilizes the NLO molecules in the direction of the electric field.

The effectiveness of corona poling and contact plate poling in aligning the NLO molecules seems to be different. Presented results indicate that contact plate poling is not as effective as corona poling, mainly because of the maximum electric voltage one can apply across the film, which is determined by the dielectric constant and other properties of the material. A linear relationship was obtained between the measured $\chi^{(2)}$ and the applied electric field, up to 2×10^6 V/cm, in the case of contact plate poling, in agreement with eq 1, which is valid only under week electric field, i.e., when $\mu E_p/5kT \ll 1$. This implies that only a small portion (less than 5%, in the case of contact plate poling) of the NLO molecules is aligned. We have not been able to measure the electric field inside the film during corona poling. But it is estimated that the field in this case is much stronger than in the case of contact plate poling. This can account for one of the reasons why the $\chi^{(2)}$ value determined by electrooptic modulation measurement is lower than the value determined from the second-harmonic generation experiment, performed on the films in which the NLO molecules are aligned by corona poling. The other reason is the dispersion of $\chi^{(2)}$.

We have achieved a $\chi^{(2)}$ value of 2.6×10^{-8} esu (10.9 pm/V) with a number density of 6×10^{20} molecules/cm^3

(15) Jerphagnon, J.; Kurtz, S. K. *J. Appl. Phys.* **1970**, *41*, 1667.

(16) Khanarian, G.; Che, T.; DeMartino, R. N.; Teng, C. C.; Yoon, H. N. *Proc. SPIE* **1987**, *824*.

of the NPP molecules in the sol–gel matrix. No crystallization of NPP molecules has been observed. The number density and the $\chi^{(2)}$ values are both considerably higher than that previously reported by Puccetti.[17]

In conclusion, we have achieved high second-order nonlinearity in a sol–gel-processed inorganic oxides:organic compound composite. The NLO active organic molecules have been aligned by an applied electric field. Both second harmonic generation and electrooptic modulation have been studied. Long-term stability of a bulk second-order

susceptibility has been obtained.

Registry No. *N*-(4-nitrophenyl)-(*s*)-prolinol, 88422-19-9; silica, 7631-86-9; titanium dioxide, 13463-67-7.

(17) Puccetti, G.; Toussaere, E.; Ledoux, I.; Zyss, J. *Polym. Prepr.* (*Am. Chem. Soc., Div. Polym. Chem.*) **1991**, *32*, 61.

Silica-Pillared Derivatives of H+-Magadiite, a Crystalline Hydrated Silica

James S. Dailey and Thomas J. Pinnavaia*

Department of Chemistry and Center for Fundamental Materials Research, Michigan State University, East Lansing, Michigan 48824

H+-magadiite ($H_4Si_{14}O_{30} \cdot H_2O$), a hydrous lamellar silicic acid formed by proton ion exchange of Na+-magadiite ($Na_{1.7}H_{1.9}Si_{14}O_{29.8} \cdot 7.7H_2O$), reacts with neat octylamine to form an octylamine/octylammonium–magadiite gel with a basal spacing (34 Å) corresponding to the presence of an intercalated bilayer of onium ions and amine molecules. Reaction of the swollen gel with neat tetraethylorthosilicate at TEOS:magadiite ratios in the range 54:1 to 154:1, followed by drying of the solid products in air, affords siloxane-intercalated derivatives with basal spacings of 23–28 Å. FTIR studies and analytical results indicate that TEOS intercalation occurs by displacement of octylamine. Also, TEM images show that the hydrolyses and condensation–polymerization of TEOS is topotactic. Calcination of the siloxane intercalates at 300 °C yields silica-pillared magadiites with basal spacings of 20.7–25.9 Å and *microporous* surface areas of 480–670 m^2/g. ^{29}Si MAS NMR results show that the overall Q^3 and Q^4 connectivity of SiO$_4$ units decreases from a ratio of 0.28 ± 0.02 for the air-dried siloxane derivatives to 0.19 ± 0.02 for the calcined silica pillared forms. Pristine H+-magadiite exhibits a Q^3/Q^4 ratio of 0.28. However, the presence of Q^2 silicon environments in the silica-pillared products precludes the possibility of the pillars being isostructural with the magadiite layers.

Introduction

Pillared layered materials have attracted widespread interest over the past 10 years due in part of their catalytic and molecular sieving properties.[1-3] In an effort to broaden the diversity of pillared lamellar materials, we and several other groups of workers have been investigating the pillaring reactions of the hydrous sodium silicate Na+-magadiite ($Na_2Si_{14}O_{29} \cdot 9H_2O$). Other examples of this unique family of silicates include kenyaite ($Na_2Si_{20}O_{41} \cdot 10H_2O$), makatite ($Na_2Si_4O_9 \cdot 5H_2O$), and kanemite ($NaHSi_2O_5 \cdot 3H_2O$). All are naturally occurring minerals, many of which are found in lake beds at Lake Magadi, Kenya.[4] These compounds also can be conveniently prepared in the laboratory by hydrothermal synthesis.[5-7]

Intercalative ion-exchange reactions of Na+-magadiite with robust cations is not a generally viable approach to synthesizing pillared derivatives, owing in part to the relatively high layer charge and limited swelling characteristics of the interlayers. For instance, our recent attempts to pillar Na+-magadiite by ion exchange of cobalt sepulchrate, [Co(sep)]$^{3+}$, a metal cage complex noted for its exceptional stability in solution,[8] afforded instead a "stuffed", nonmicroporous intercalated derivative in which one-half of the metal centers were no longer complexed by the sepulchrate ligand.[9] Also, Fripiat and co-workers[10] have found that $KHSi_2O_5$, a related layer silicate, undergoes ion-exchange reaction with $Al_{13}O_4(OH)_{24}(H_2O)_{12}^{7+}$ cations, but the products are highly disordered.

The intercalation of grafted silyl groups in layered silicates appears to be a more promising approach to ordered

(1) Figueras, F. *Catal. Rev.* **1988**, *30*, 457.
(2) Vaughan, D. E. W. In *Perspectives in Molecular Sieve Science*; Flank, W. H., Whyte, T. E., Eds.; American Chemical Society: Washington, DC, 1988; p 308.
(3) *Pillared Layered Structures: Current Trends and Applications*; Mitchell, I. V., Ed.; Elsevier: New York, 1990.
(4) Eugster, H. P. *Science* **1967**, *157*, 1177.
(5) Fletcher, R. A.; Bibby, D. M. *Clays Clay Miner.* **1987**, *35*, 318.
(6) Beneke, K.; Lagaly, G. *Am. Miner.* **1983**, *68*, 818; **1977**, *62*, 763.

(7) Schwieger, W.; Heyer, W.; Wolf, F.; Bergk, K.-H. *Z. Anorg. Allg. Chem.* **1987**, *548*, 204.
(8) Creaser, I. I.; Geue, R. J.; Harrowfield, J. M.; Herlt, A. J.; Sargeson, A. M.; Snow, M. R.; Springborg, J. *J. Am. Chem. Soc.* **1982**, *104*, 6016.
(9) Dailey, J. S.; Pinnavaia, T. J. *J. Inclusion Phenom.*, in press.
(10) Deng, Z.; Lambert, J. F. H.; Fripiat, J. J. *Chem. Mater.* **1989**, *1*, 640.